

Published in final edited form as:

*J Hepatol.* 2010 April ; 52(4): 586–593. doi:10.1016/j.jhep.2010.01.003.

## Palmitoleate attenuates palmitate-induced bim and PUMA up-regulation and hepatocyte lipoapoptosis

Yuko Akazawa<sup>1,2</sup>, Sophie Cazanave<sup>1</sup>, Justin L. Mott<sup>1</sup>, Nafisa Elmi<sup>1</sup>, Steven F. Bronk<sup>1</sup>, Shigeru Kohno<sup>2</sup>, Michael R. Charlton<sup>1</sup>, and Gregory J. Gores<sup>1</sup>

<sup>1</sup>Division of Gastroenterology and Hepatology, Mayo Clinic College of Medicine, 200 First Street SW, Rochester, MN 55905, USA

<sup>2</sup>Second Department of Internal Medicine, Nagasaki University School of Medicine, Nagasaki 852-8562, Japan

### Abstract

**Background & Aims**—Saturated free fatty acids induce hepatocyte lipoapoptosis. This lipotoxicity involves an endoplasmic reticulum stress response, activation of JNK, and altered expression and function of Bcl-2 proteins. The mono-unsaturated free fatty acid, palmitoleate is an adipose-derived lipokine, which suppresses free fatty acid-mediated lipotoxicity by unclear mechanisms. Herein we examined the mechanisms responsible for cytoprotection.

**Methods**—We employed isolated human and mouse primary hepatocytes, and the Huh-7 and Hep 3B cell lines for these studies. Cells were incubated in presence and absence of palmitate (16:0), stearate (18:0), and or palmitoleate (16:1, n-7).

**Results**—Palmitoleate significantly reduced lipoapoptosis by palmitate or stearate in both primary cells and cell lines. Palmitoleate accentuated palmitate-induced steatosis in Huh-7 cells excluding inhibition of steatosis as a mechanism for reduced apoptosis. Palmitoleate inhibited palmitate induction of the endoplasmic reticulum stress response as demonstrated by reductions in CHOP expression, eIF2- $\alpha$  phosphorylation, XBP-1 splicing, and JNK activation. Palmitate increased expression of the BH3-only proteins PUMA and Bim, which was attenuated by palmitoleate. Consistent with its inhibition of PUMA and Bim induction, palmitoleate prevented activation of the downstream death mediator Bax.

**Conclusions**—These data suggest palmitoleate inhibits lipoapoptosis by blocking endoplasmic reticulum stress-associated increases of the BH3-only proteins Bim and PUMA.

### Keywords

Apoptosis; Bcl-2 proteins; Endoplasmic reticulum stress; Human hepatocytes; Nile Red, Steatosis

---

© 2010 European Association of the Study of the Liver. Published by Elsevier B.V. All rights reserved.

Corresponding author: Gregory J. Gores, Tel.: +1 507 284 0686; fax: +1 507 284 0762, gores.gregory@mayo.edu (G.J. Gores).

**Publisher's Disclaimer:** This is a PDF file of an unedited manuscript that has been accepted for publication. As a service to our customers we are providing this early version of the manuscript. The manuscript will undergo copyediting, typesetting, and review of the resulting proof before it is published in its final citable form. Please note that during the production process errors may be discovered which could affect the content, and all legal disclaimers that apply to the journal pertain.

The authors have no potential conflict of reference in regards to this manuscript.

## Introduction

The metabolic syndrome, characterized by obesity and insulin resistance, is associated with elevated levels of circulating free fatty acid (FFA) [1,2]. The excess serum FFA in the context of insulin resistance saturates the transport and storage capacity of adipocytes leading to their uptake by liver, skeletal muscle, heart, and pancreatic  $\beta$ -cells [2]. The surfeit of FFA results in their participation in non-oxidative pathways with potential deleterious consequences for the non-adipocyte including cellular demise, termed lipoapoptosis [3]. This phenomenon is particularly relevant to the liver where hepatocyte lipotoxicity contributes to the syndrome of nonalcoholic fatty liver disease (NAFLD) [4]. Indeed, hepatocyte lipoapoptosis is a pathologic feature of NAFLD and correlates with disease severity [5,6]. Thus, mechanistic insights regarding the initiation and prevention of hepatocyte lipoapoptosis are of biomedical interest.

Intracellular FFA are trafficked to and esterified within the endoplasmic reticulum (ER), and not surprisingly, inundation of the liver with FFA disturbs ER function resulting in an ER stress response [7], which is well documented in NAFLD [8]. A potent transducer of ER stress response in NAFLD is PERK [9]. PERK activation induces a transcription factor CHOP [10], which is increased in liver and hepatocytes from dietary models of hepatic steatosis [11]. Another transducer of ER stress is IRE1, which leads to activation of JNK [10]. Consistent with an ER stress-induced pathway of FFA-mediated cytotoxicity, hepatocyte lipoapoptosis is also associated with JNK activation in both rodent and human steatohepatitis, and JNK inhibition attenuates lipoapoptosis in these models [12,13]. Thus, ER stress-associated JNK activation is a potential cellular mechanism contributing to hepatocyte lipoapoptosis. Bcl-2 protein family member can act to induce or prevent apoptosis [14]. JNK activation can be linked to dysregulation of this core cell death machinery, promoting cell death [4]. In particular, JNK-1, but not JNK-2 activation by toxic FFA results in increased cellular levels of the proapoptotic BH3-only protein members of the Bcl-2 protein PUMA and silencing this death mediator attenuates lipoapoptosis [15]. JNK is also known to activate Bim [16], which is another BH3-only protein contributing to lipoapoptosis [12]. Thus, ER stress can be directly coupled to dysregulation of Bcl-2 proteins which in turn trigger the mitochondrial pathway of apoptosis. Taken together, these observations suggest FFA induce lipoapoptosis through both induction of PUMA and Bim, which in turn result in activation of the downstream death mediator Bax. Oligomerization of Bax within the outer mitochondrial membrane triggers mitochondrial dysfunction and cell death [17].

FFA and not their esterified product (triglyceride) appear to mediate lipotoxicity [18]. Experimental evidence indicate that saturated FFA such as PA (a 16 carbon FFA with no carbon-carbon double bonds, indicated 16:0) and stearate (18:0; SA) are more toxic than unsaturated FFA [12]. The mono-unsaturated FFA palmitoleate (PO; 16:1n-7), is a unique product of adipocytes and functions as a lipid hormone, called a lipokine [19]. Although PO itself may effect minimal cytotoxicity, it is far less compared to saturated free fatty acids [12]. Furthermore, PO exerts a salutary effect in a murine model of the metabolic syndrome [19], in part, by reducing expression of SCD-1, an enzyme which converts saturated FFA into monounsaturated FFA; a key step in channeling FFA into triglyceride synthesis [20]. PO has also been reported to reduce toxic FFA acid-induced apoptosis in rat hepatoma cell lines [21]. However, the mechanisms by which PO exerts its cytoprotective effects remain unclear and have not been directly examined in human hepatocytes. An understanding of how this lipokine mitigates hepatocyte lipoapoptosis may help identify treatment strategies for human NAFLD.

The current work addresses the question of how PO reduces hepatocyte lipoapoptosis by toxic saturated FFA *in vitro*. We identify a pathway that involves PO inhibition of ER stress, and

PUMA and Bim induction by PA. Inhibition of ER stress-mediated dysregulation of Bim and PUMA by PO and/or analogues may be salutary in human NAFLD.

## Materials and methods

### Cells

The human hepatocellular carcinoma cell lines, Huh-7, and Hep3B cells and primary hepatocytes were employed for these studies. Detailed information regarding the culture conditions are in the supplementary materials and methods section.

### Fatty acid treatment

Palmitic acid (catalog # P5585) and palmitoleic acid (catalog # P9417) were obtained from Sigma-Aldrich (St. Louis, MO). Free fatty acids were dissolved in isopropanol at a concentration of 20 to 80 mM. FFA were added to DMEM containing 1% bovine serum albumin to assure a physiologic ratio between bound and unbound FFA in the media [22]. The concentration of individual FFA used in the experiments (200–800  $\mu$ M) are similar to the fasting total FFA plasma concentrations observed in human nonalcoholic steatohepatitis [23–25].

### Quantification of apoptosis

Apoptosis was quantified by assessing the characteristic nuclear changes of apoptosis using the nuclear binding dye DAPI (Molecular Probes, Eugene, OR) and fluorescence microscopy (Zeiss LSM 510, Carl Zeiss, Jena, Germany). Caspase 3/7 activation in cell cultures was measured using Apo-ONE homogeneous caspase 3/7 kit (Promega, Madison, WI) according to the manufacturer's instructions.

### Nile Red staining

Huh-7 cells were grown on glass coverslips. Intracellular neutral lipid was stained with Nile Red (1  $\mu$ g/ml) for 5 min at room temperature. Cells were then fixed with 3.7% paraformaldehyde for 15 min at room temperature. After washing with PBS, cells were mounted in Prolong Antifade (Invitrogen, Camarillo, CA) and visualized using an inverted laser-scanning confocal microscope (Zeiss LSM 510, Carl Zeiss, Jena, Germany) with wavelength of 480 nm for excitation and greater than 505 nm for emission for lipid stain [26]. Cellular fluorescence was quantitated using Zeiss KS400 image analysis software (Carl Zeiss, Inc., Oberkochen, Germany) and expressed as percent of Nile red positive area per cell.

### Real time polymerase chain reaction (PCR)

Total RNA was extracted from the cells using the Trizol reagent (Invitrogen) and was reverse-transcribed into complementary DNA with Moloney murine leukemia virus reverse transcriptase (Invitrogen) and random primers (Invitrogen). Quantification of the complementary DNA template was performed with real time PCR (LightCycler; Roche Applied Science) using SYBR green (Molecular Probes) as a fluorophore. PCR primers were as follows: for human SCD-1 forward (5'-CGCTAGACTTGTCTGACCTAGAA-3') and reverse (5'-CAAGCGTGGGCAGGATGAAGCA-3'), for human PUMA forward (5'-GACGACCTCAACGCACAGTA-3') and reverse (5'-AGGAGTCCCATGATGAGATTGT-3'), and for human GADD 34 forward (5'-CGACTGCAAAGGCGGC-3') and reverse (5'-CAGGAAATGGACAGTGACCTTCT-3'). As an internal control, primers for 18S ribosomal RNA (rRNA) were used (Ambion, Austin, TX). The relative mRNA expression levels were expressed as a ratio of target mRNA /18S rRNA per each sample as previously described by us in detail [27]. CHOP real time PCR was

performed using Taqman technology using commercially available primers (Hs00358796\_g1) from Applied Biosystems.

### Immunoblot analysis

Whole cell lysates were prepared and subjected to immunoblot analysis as previously described in detail [27]. For CHOP protein analysis, nuclear extract from whole cell lysates were obtained using Nuclear and Cytoplasmic Extraction Reagent (Thermo Scientific, Rockford, IL) following manufacturer's instruction. Samples containing 60  $\mu$ g protein were resolved by 4–15% SDS-PAGE, transferred to nitrocellulose membranes, and incubated with primary antibodies at a dilution of 1:1000. Membranes were incubated with appropriate horseradish peroxidase-conjugated secondary antibodies (Biosource International, Camarillo, CA) at a dilution of 1:3000. Bound antibody was visualized using chemiluminescent substrate (ECL, Amersham, Arlington Heights, IL) and was exposed to Kodak XOMAT film (Eastman Kodak, Rochester, NY).

### Immunocytochemistry for Bax activation

Immunocytochemistry of activated Bax was performed using mouse anti-universal Bax (clone 6A7, 1:300 dilution, Exalpha Biologicals, Watertown, MA) as previously described in detail [15].

Detailed information on cells cultures and conditions, antibodies and reagents, analysis of XBP-1 splicing and statistical analysis are in the Supplemental Materials and methods.

## Results

### Despite accentuating cellular steatosis, PO attenuates PA-mediated lipoapoptosis

We have previously reported that PA treatment of hepatocytes is associated with cellular steatosis [12], therefore, we initially examined the effect of PO on PA-associated cellular steatosis in Huh-7 cells. Cells were treated with either vehicle, 200  $\mu$ M of PA, 200  $\mu$ M of PO, or a combination of both. Unexpectedly, the magnitude of cellular steatosis was even greater with PO than PA (Figure 1A,B). The combination resulted in steatosis similar to that observed with PO alone. Although PO is thought to inhibit hepatic steatosis *in vivo* by reducing SCD-1 expression [19], PO did not alter expression of SCD-1 mRNA in Huh-7 cells *in vitro* (PA 800  $\mu$ M, PO 400  $\mu$ M) (Figure 1C). Thus, PO does not reduce the intracellular accumulation of neutral lipids when cells are incubated with PA but rather increases steatosis in cultured Huh-7 cells. Despite promoting increased lipid accumulation, PO attenuates PA-induced apoptosis. As maximal cytoprotective effect was observed at a PA:PO ratio of 2:1 in Huh-7 cells, and 1:1 in other liver cell lines and primary hepatocytes, these ratios were employed for all further studies (data not shown). As assessed by morphologic criteria, PO reduced PA-mediated apoptosis in Huh-7 (PA 800  $\mu$ M, PO 400  $\mu$ M) and Hep 3B cell lines (PA 400  $\mu$ M, PO 400  $\mu$ M), and primary mouse and human hepatocytes (PA 400  $\mu$ M, PO 400  $\mu$ M) (Figure 2A). This cytoprotective effect of PO was dose-dependent (Supplemental Figure 1). Apoptosis was also confirmed biochemically in Huh-7 cells and Hep 3B cells as examined by measuring caspase 3/7 activity which yielded results virtually identical to the morphologic studies (Figure 2B). This anti-apoptotic effect of PO was also observed in stearate (SA)-treated cells (SA 800  $\mu$ M, PO 400  $\mu$ M) (Supplemental Figure 2A, B). Taken together, these data indicate that PO potently suppresses saturated FFA cytotoxicity despite enhancing steatosis. Given that PO cytoprotection was similar in cell lines and primary hepatocytes, we employed the Huh-7 cell line for further mechanistic studies.

### PO attenuates ER stress-induced by PA

Previous work by Pagliassotti and coworkers indicates that FFA-induced lipoapoptosis occurs via an ER-stress pathway [8]. Therefore we explored the effect of PO on ER stress-induced by PA. First, we examined activation of the PERK response system of the ER stress pathway [10], which is characterized by CHOP induction [28]. PA-mediated induction of CHOP mRNA and protein expression was reduced in the presence of PO (Figure 3A and 3B). PO also attenuated induction of GADD 34 mRNA, which is also up-regulated by ER stress downstream of CHOP [10] (Supplemental Figure 3). Furthermore, PO also attenuated phosphorylation of eIF2- $\alpha$ , which is also activated by PERK [10] (Figure 3C). Next, we examined the ER stress response transduced by IRE-1, which is characterized by XBP-1 splicing and JNK activation [10]. PA treatment of Huh-7 cells induced XBP-1 splicing, consistent with activation of IRE-1 endonuclease activity (Figure 4A). This XBP-1 splicing was inhibited by PO (PA 800  $\mu$ M, PO 400  $\mu$ M) (Figure 4A). Activating phosphorylation of JNK by PA was also reduced in the presence of PO (PA 800  $\mu$ M, PO 400  $\mu$ M) (Figure 4B). These results indicate that PO inhibits multiple ER stress pathways initiated by PA. Finally, we ascertained if PO also reduces ER stress by thapsigargin or tunicamycin, which are classic cell biological approaches for inducing ER stress [29]. PO did not, however, inhibit thapsigargin nor tunicamycin-induced CHOP mRNA expression (Supplemental Figure 4). Collectively, these data indicate that PO blocks ER stress by PA, an effect specific for cytotoxic FFA.

### PO reduces Bim and PUMA induction, and Bax activation by PA

Consistent with our previous observation [15,27], PA increased PUMA and Bim cellular protein levels (Figure 5A). In contrast, cellular levels of other BH3-only proteins (Noxa, Bik, Bad, Bid), pro-apoptotic multidomain Bcl-2 proteins (Bak, Bax), and the anti-apoptotic protein Bcl-X<sub>L</sub> were unaltered. Consistent with its cytoprotective effects, PO (PO 400 $\mu$ M and PA 400 $\mu$ M) attenuated Bim and PUMA induction by PA. In addition, PO also attenuated PUMA mRNA induction by PA (Figure 5B). Activation of Bax, a known mediator of mitochondrial dysfunction, is required for induction of hepatocyte lipoapoptosis downstream of PUMA and Bim induction [12,15]. Indeed, both Bim and PUMA can directly activate Bax which in turn triggers mitochondrial dysfunction and cell death [14]. Activated Bax was identified by immunofluorescence using the 6A7 monoclonal antibody which detects the active conformational form of Bax [30]. Consistent with previous reports [12,15], Bax activation was observed in PA-treated cells, but this activation was attenuated when cells were incubated with PA plus PO (PA 800  $\mu$ M, PO 400  $\mu$ M) (Figure 5C). Taken together, the data suggest the inhibition of ER stress by PO also prevents dysregulation of Bcl-2 proteins by cytotoxic FFA.

## Discussion

Results of the present study provide new insights into the mechanisms of PO cytoprotection during FFA-induced lipoapoptosis. The principal findings of this study indicate that: i) PO does not attenuate steatosis *in vitro*; ii) PO inhibits saturated FFA-induced apoptosis in hepatocytes; iii) PO inhibits PA-induced ER stress; and iv) PO inhibits PA-induced dysregulation of pro-apoptotic Bcl-2 proteins. Each of these results is discussed in greater detail below.

A recent study suggested PO may function as a lipokine, a circulating lipid mediator, which modulates insulin sensitivity both in liver and muscle. Although PO accounts for a minority of the circulating FFA in healthy and in NASH patients, it is a potent signalling molecule [19,31]. For example, at physiological concentrations, PO improves the metabolic syndrome in a murine model, in part, by reducing hepatic SCD-1 [19]. In our reductionistic, cell culture model, PO actually promoted steatosis and had no effect on SCD-1 expression. These data suggest that SCD-1 expression in hepatocytes is not directly regulated by PO.

Despite promoting increased cellular steatosis, PO was cytoprotective during PA-mediated lipoapoptosis. This is consistent with prior observations reporting that unsaturated FFA are more efficiently esterified and incorporated into triglycerides [32]. Unsaturated FFA promote triglyceride generation likely due to their increased fluidity which facilitates their incorporation into lipid droplets [32]. Efficient incorporation of FFA within neutral lipids appears to be a detoxification process minimizing the inherent toxicity of FFA [8,18]. These concepts help explain, in part, the increased triglyceride accumulation in PO-treated cells and PO's ability to mitigate PA toxicity. In fact, other unsaturated FFA such as oleic acid and linoleic acid also inhibit cytotoxicity and ER stress by saturated FFA [8,29,33]. In this respect, the cytoprotective effects of PO mimic those of other unsaturated FFA [33]. Our studies extend the concept of cytoprotection by unsaturated FFA, by demonstrating PO cytoprotection in primary human hepatocytes, an important translational research observation. The observation that human hepatocytes undergo lipoapoptosis by PA and PO is cytoprotective in this paradigm helps, in part, validate prior studies of lipoapoptosis in hepatocyte derived cell lines and primary rodent hepatocyte cultures. Involvement of ER stress has been implicated in saturated FFA-mediated apoptosis in liver cells [8,29], and saturated FFA, but not unsaturated FFA induce ER stress *in vivo* [11]. Our current results indicate that PO inhibits induction of a pivotal ER stress markers, in particular CHOP induction. This mediator of ER stress has been implicated in multiple models of ER stress-associated apoptosis. For example, ER stress-induced apoptosis is reduced in CHOP knockout mouse compared to wild type animals [34]. Genetic deletion of CHOP also reduces Bim induction during ER stress [35]. These and our current observations suggest that Bim induction during lipotoxicity is due to downstream ER stress.

We note that in our present study, PO did not inhibit thapsigargin nor tunicamycin-induced CHOP up-regulation in Huh-7 cells. These data indicate that PO is not a general inhibitor of the ER stress response, but rather specifically antagonizes ER stress-induction by cytotoxic FFA. This information implies that ER stress is not a single, standardized signal, but rather that it is due to different activators that act through individualized, specific pathways. Further studies are necessary to identify how FFA modulate this unique ER stress response.

Prior studies on lipoapoptosis have not delineated the downstream consequences of FFA-mediated ER stress. PO attenuation of the ER stress response permits further dissection of these downstream events. A key downstream mediator of ER stress is JNK which has been implicated in human and murine steatohepatitis [36]. For example, prior studies have highlighted the importance of JNK-1 activation leading to PUMA protein induction during lipoapoptosis [15]. In these studies, genetic knockdown of PUMA attenuates hepatocyte lipoapoptosis [15]. The current study extends these observations by demonstrating that inhibition of ER stress with PO attenuates this JNK-dependent dysregulation of pro-apoptotic Bcl-2 proteins. These cytotoxic responses to saturated FFA appear to be downstream of ER stress. An emerging picture of lipoapoptosis is developing with ER stress upstream of JNK activation which then, likely in concert with other mediators, such as CHOP, contributes to increased PUMA transcription and Bim activation [35]. These BH3-only proteins then trigger Bax activation resulting in the mitochondrial pathway of cell death (Figure 6). Collectively, our present findings suggest that the lipokine PO attenuates saturated FFA-induced cell death in hepatocytes by inhibiting ER stress-associated dysregulation of pro-apoptotic Bcl-2 proteins. These data link PO cytoprotection to a beneficial effect on the core-apoptotic machinery of the cell. Given this mechanistic insight, it is tempting to speculate that PO and/or potent PO analogues could prove beneficial in human NAFLD.

## Supplementary Material

Refer to Web version on PubMed Central for supplementary material.

## Acknowledgments

The authors who have taken part in this study declared that they do not have anything to declare regarding funding from industry or conflict of interest with respect to this manuscript. This work was supported by NIH Grants DK 41876 to GJG, DK 79875 to JLM, DK 69757 to MRC, the Optical Microscopy Core of P30 DK 84567, and the Mayo Foundation. We thank Dr. Anuradha Krishnan and Kimberly B. Viker for isolating the human primary hepatocytes, and Erin Nystuen-Bungum for her excellent secretarial assistance.

## Abbreviations

FFA	free fatty acid
NAFLD	nonalcoholic fatty liver disease
ER	endoplasmic reticulum
PERK	protein kinase RNA-like ER kinase
CHOP	CCAAT/enhancer binding homologous protein
IRE-1	inositol-requiring protein-1
JNK	c-Jun-N-terminal kinase
BH3	Bcl-2 homology 3
PUMA	p53-upregulated mediator of apoptosis
Bim	Bcl-2-interacting mediator of cell death
PA	palmitate
SA	stearate
PO	palmitoleate
SCD-1	stearoyl-CoA desaturase-1
DMEM	Dulbecco's modified Eagle's medium with high glucose
PCR	polymerase chain reaction
GADD 34	growth arrest and DNA damage gene 34
Bax	BCL2-associated Xprotein
XBP-1	X Box binding protein-1
eIF2- $\alpha$	eukaryotic initiation factor 2-alpha
DAPI	4',6-diamidino-2-phenylindole

## References

1. Angulo P. Nonalcoholic fatty liver disease. *N Engl J Med* 2002;346:1221–1231. [PubMed: 11961152]
2. Parekh S, Anania FA. Abnormal lipid and glucose metabolism in obesity: implications for nonalcoholic fatty liver disease. *Gastroenterology* 2007;132:2191–2207. [PubMed: 17498512]
3. Unger RH, Orci L. Lipoapoptosis: its mechanism and its diseases. *Biochim Biophys Acta* 2002;1585:202–212. [PubMed: 12531555]
4. Malhi H, Gores GJ. Molecular mechanisms of lipotoxicity in nonalcoholic fatty liver disease. *Semin Liver Dis* 2008;28:360–369. [PubMed: 18956292]
5. Feldstein AE, Gores GJ. Apoptosis in alcoholic and nonalcoholic steatohepatitis. *Front Biosci* 2005;10:3093–3099. [PubMed: 15970563]

6. Feldstein AE, Canbay A, Angulo P, Taniai M, Burgart LJ, Lindor KD, et al. Hepatocyte apoptosis and fas expression are prominent features of human nonalcoholic steatohepatitis. *Gastroenterology* 2003;125:437–443. [PubMed: 12891546]
7. Gregor MG, Hotamisligil GS. Adipocyte stress: The endoplasmic reticulum and metabolic disease. *J Lipid Res.* 2007 May 9;
8. Wei Y, Wang D, Topczewski F, Pagliassotti MJ. Saturated fatty acids induce endoplasmic reticulum stress and apoptosis independently of ceramide in liver cells. *Am J Physiol Endocrinol Metab* 2006;291:E275–E281. [PubMed: 16492686]
9. Puri P, Mirshahi F, Cheung O, Natarajan R, Maher JW, Kellum JM, et al. Activation and dysregulation of the unfolded protein response in nonalcoholic fatty liver disease. *Gastroenterology* 2008;134:568–576. [PubMed: 18082745]
10. Ron D, Walter P. Signal integration in the endoplasmic reticulum unfolded protein response. *Nat Rev Mol Cell Biol* 2007;8:519–529. [PubMed: 17565364]
11. Wang D, Wei Y, Pagliassotti MJ. Saturated fatty acids promote endoplasmic reticulum stress and liver injury in rats with hepatic steatosis. *Endocrinology* 2006;147:943–951. [PubMed: 16269465]
12. Malhi H, Bronk SF, Werneburg NW, Gores GJ. Free fatty acids induce JNK-dependent hepatocyte lipoapoptosis. *J Biol Chem* 2006;281:12093–12101. [PubMed: 16505490]
13. Schattenberg JM, Singh R, Wang Y, Lefkowitz JH, Rigoli RM, Scherer PE, et al. JNK1 but not JNK2 promotes the development of steatohepatitis in mice. *Hepatology* 2006;43:163–172. [PubMed: 16374858]
14. Youle RJ, Strasser A. The BCL-2 protein family: opposing activities that mediate cell death. *Nat Rev Mol Cell Biol* 2008;9:47–59. [PubMed: 18097445]
15. Cazanave SC, Mott JL, Elmi NA, Bronk SF, Werneburg NW, Akazawa Y, et al. JNK1-dependent PUMA expression contributes to hepatocyte lipoapoptosis. *J Biol Chem* 2009;284:26591–26602. [PubMed: 19638343]
16. Dhanasekaran DN, Reddy EP. JNK signaling in apoptosis. *Oncogene* 2008;27:6245–6251. [PubMed: 18931691]
17. Taylor RC, Cullen SP, Martin SJ. Apoptosis: controlled demolition at the cellular level. *Nat Rev Mol Cell Biol* 2008;9:231–241. [PubMed: 18073771]
18. Yamaguchi K, Yang L, McCall S, Huang J, Yu XX, Pandey SK, et al. Inhibiting triglyceride synthesis improves hepatic steatosis but exacerbates liver damage and fibrosis in obese mice with nonalcoholic steatohepatitis. *Hepatology* 2007;45:1366–1374. [PubMed: 17476695]
19. Cao H, Gerhold K, Mayers JR, Wiest MM, Watkins SM, Hotamisligil GS. Identification of a lipokine, a lipid hormone linking adipose tissue to systemic metabolism. *Cell* 2008;134:933–944. [PubMed: 18805087]
20. Miyazaki M, Kim YC, Gray-Keller MP, Attie AD, Ntambi JM. The biosynthesis of hepatic cholesterol esters and triglycerides is impaired in mice with a disruption of the gene for stearoyl-CoA desaturase 1. *J Biol Chem* 2000;275:30132–30138. [PubMed: 10899171]
21. Yamasaki M, Chujo H, Nou S, Tachibana H, Yamada K. Alleviation of the cytotoxic activity induced by trans10, cis12-conjugated linoleic acid in rat hepatoma dRLh-84 cells by oleic or palmitoleic acid. *Cancer Lett* 2003;196:187–196. [PubMed: 12860277]
22. Richieri GV, Kleinfeld AM. Unbound free fatty acid levels in human serum. *J Lipid Res* 1995;36:229–240. [PubMed: 7751810]
23. Sanyal AJ, Campbell-Sargent C, Mirshahi F, Rizzo WB, Contos MJ, Sterling RK, et al. Nonalcoholic steatohepatitis: association of insulin resistance and mitochondrial abnormalities. *Gastroenterology* 2001;120:1183–1192. [PubMed: 11266382]
24. Belfort R, Harrison SA, Brown K, Darland C, Finch J, Hardies J, et al. A placebo-controlled trial of pioglitazone in subjects with nonalcoholic steatohepatitis. *N Engl J Med* 2006;355:2297–2307. [PubMed: 17135584]
25. Nehra V, Angulo P, Buchman AL, Lindor KD. Nutritional and metabolic considerations in the etiology of nonalcoholic steatohepatitis. *Dig Dis Sci* 2001;46:2347–2352. [PubMed: 11713934]
26. Greenspan P, Mayer EP, Fowler SD. Nile red: a selective fluorescent stain for intracellular lipid droplets. *J Cell Biol* 1985;100:965–973. [PubMed: 3972906]



27. Barreiro FJ, Kobayashi S, Bronk SF, Werneburg NW, Malhi H, Gores GJ. Transcriptional regulation of Bim by FoxO3A mediates hepatocyte lipoapoptosis. *J Biol Chem* 2007;282:27141–27154. [PubMed: 17626006]
28. Wang XZ, Lawson B, Brewer JW, Zinszner H, Sanjay A, Mi LJ, et al. Signals from the stressed endoplasmic reticulum induce C/EBP-homologous protein (CHOP/GADD153). *Mol Cell Biol* 1996;16:4273–4280. [PubMed: 8754828]
29. Wei Y, Wang D, Gentile CL, Pagliassotti MJ. Reduced endoplasmic reticulum luminal calcium links saturated fatty acid-mediated endoplasmic reticulum stress and cell death in liver cells. *Mol Cell Biochem* 2009;331:31–40. [PubMed: 19444596]
30. Hsu YT, Youle RJ. Nonionic detergents induce dimerization among members of the Bcl-2 family. *J Biol Chem* 1997;272:13829–13834. [PubMed: 9153240]
31. Puri P, Baillie RA, Wiest MM, Mirshahi F, Choudhury J, Cheung O, et al. A lipidomic analysis of nonalcoholic fatty liver disease. *Hepatology* 2007;46:1081–1090. [PubMed: 17654743]
32. Listenberger LL, Han X, Lewis SE, Cases S, Farese RV Jr, Ory DS, et al. Triglyceride accumulation protects against fatty acid-induced lipotoxicity. *Proc Natl Acad Sci U S A* 2003;100:3077–3082. [PubMed: 12629214]
33. Maedler K, Oberholzer J, Bucher P, Spinas GA, Donath MY. Monounsaturated fatty acids prevent the deleterious effects of palmitate and high glucose on human pancreatic beta-cell turnover and function. *Diabetes* 2003;52:726–733. [PubMed: 12606514]
34. Zinszner H, Kuroda M, Wang X, Batchvarova N, Lightfoot RT, Remotti H, et al. CHOP is implicated in programmed cell death in response to impaired function of the endoplasmic reticulum. *Genes Dev* 1998;12:982–995. [PubMed: 9531536]
35. Puthalakath H, O'Reilly LA, Gunn P, Lee L, Kelly PN, Huntington ND, et al. ER stress triggers apoptosis by activating BH3-only protein Bim. *Cell* 2007;129:1337–1349. [PubMed: 17604722]
36. Singh R, Wang Y, Xiang Y, Tanaka KE, Gaarde WA, Czaja MJ. Differential effects of JNK1 and JNK2 inhibition on murine steatohepatitis and insulin resistance. *Hepatology* 2009;49:87–96. [PubMed: 19053047]

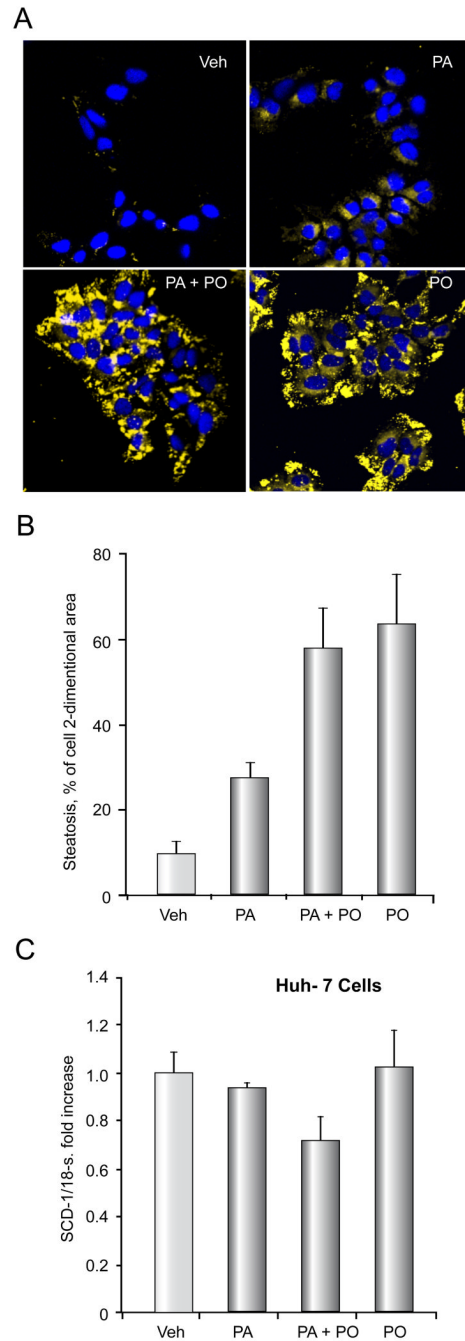


**Figure 1. PO does not attenuate PA- mediated steatosis**

Nile red staining was performed on Huh-7 cells treated with vehicle (Veh), 200  $\mu$ M PA, 200  $\mu$ M PO plus 200  $\mu$ M PA, or 200  $\mu$ M PO alone for 18 h. (A) Representative fluorescent photomicrographs ( $\times 60$ ) are depicted. Nile red fluoresces as a yellow-gold at about 510nm; cells were counter-stained for nucleic acids by DAPI (blue). (B), Cellular steatosis was quantified in 5 random low power fields for each condition with image analysis software. Total area of lipid per cell (pixels above threshold) is represented. The data represent the mean  $\pm$  SEM for n = 3 studies. (C) Huh-7 cells were treated with vehicle (Veh), 800  $\mu$ M PA, 400  $\mu$ M PO plus 800  $\mu$ M PA, or 400  $\mu$ M PO alone for 8 hours. SCD-1 mRNA was quantified by real

time PCR. Fold induction was determined by normalization to 18S ribosomal RNA. Data represent the mean  $\pm$  SEM of 3 independent experiments.

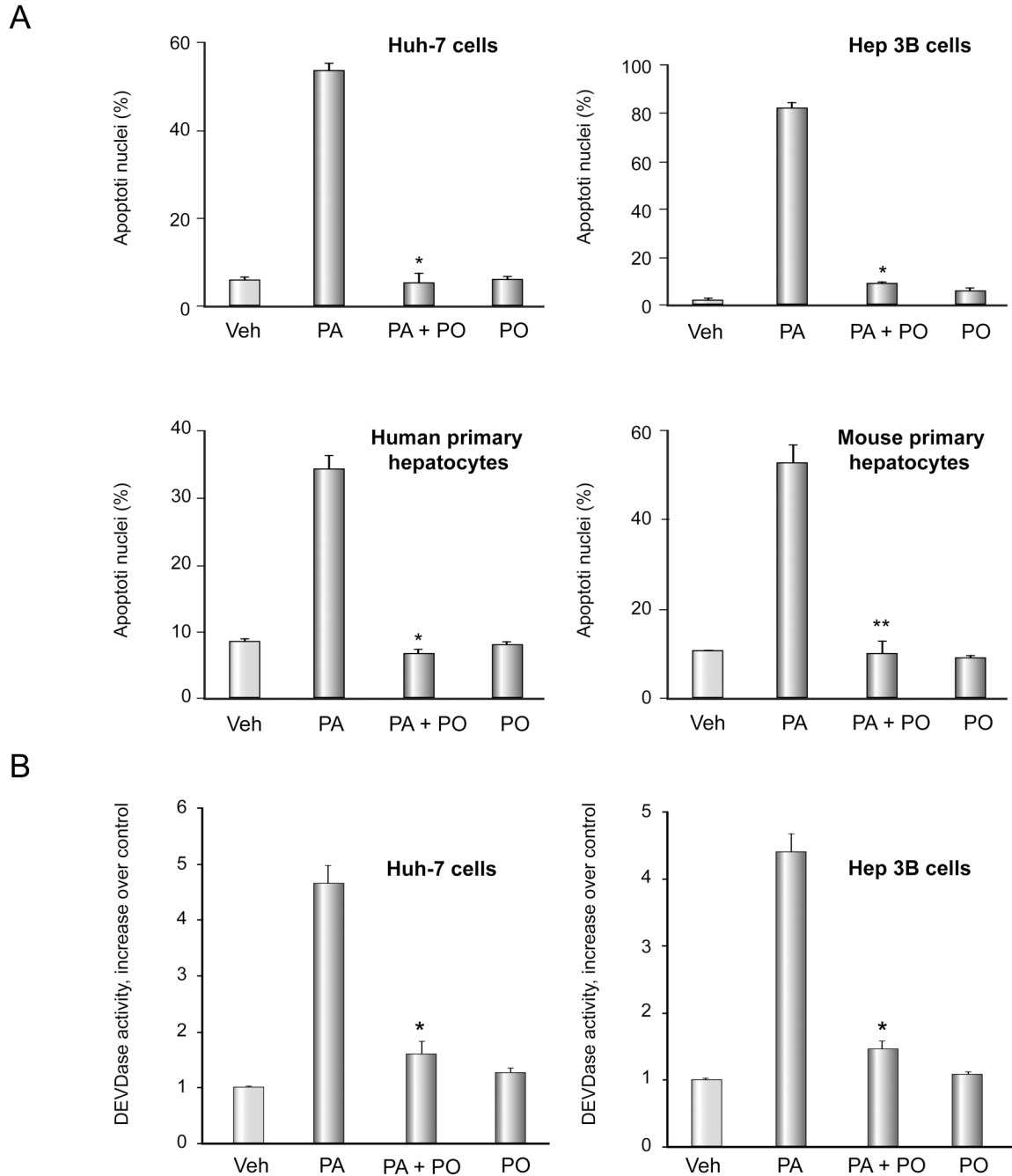


**Figure 2. PO attenuates PA-mediated apoptosis**

(A) Cells were treated with free fatty acids. The concentration of PA was 800  $\mu$ M for Huh-7 cell, 400  $\mu$ M for Hep 3B cells and 200  $\mu$ M for primary hepatocytes. The ratio of PA: PO was 2:1 for Huh-7 cells and 1:1 for the remainder of the cell types. Apoptosis was assessed by morphological criteria after DAPI staining. The data represent the mean  $\pm$  SEM for  $n = 3$  studies. \*  $p < 0.01$ , \*\*  $p < 0.05$ , PA-treated cells vs. PA plus PO-treated cells. (B) After Huh-7 cells were treated as in (A), activity of effector caspases 3 and 7 was measured by a fluorogenic assay. Data are expressed as fold-increase of relative fluorescence units (RFLU) over control value (untreated cells), which was arbitrarily set to 1, and represent the mean  $\pm$  SEM for  $n=3$  studies each performed in triplicate. \*  $p < 0.05$ , PA-treated cells vs. PA plus PO-treated cells.

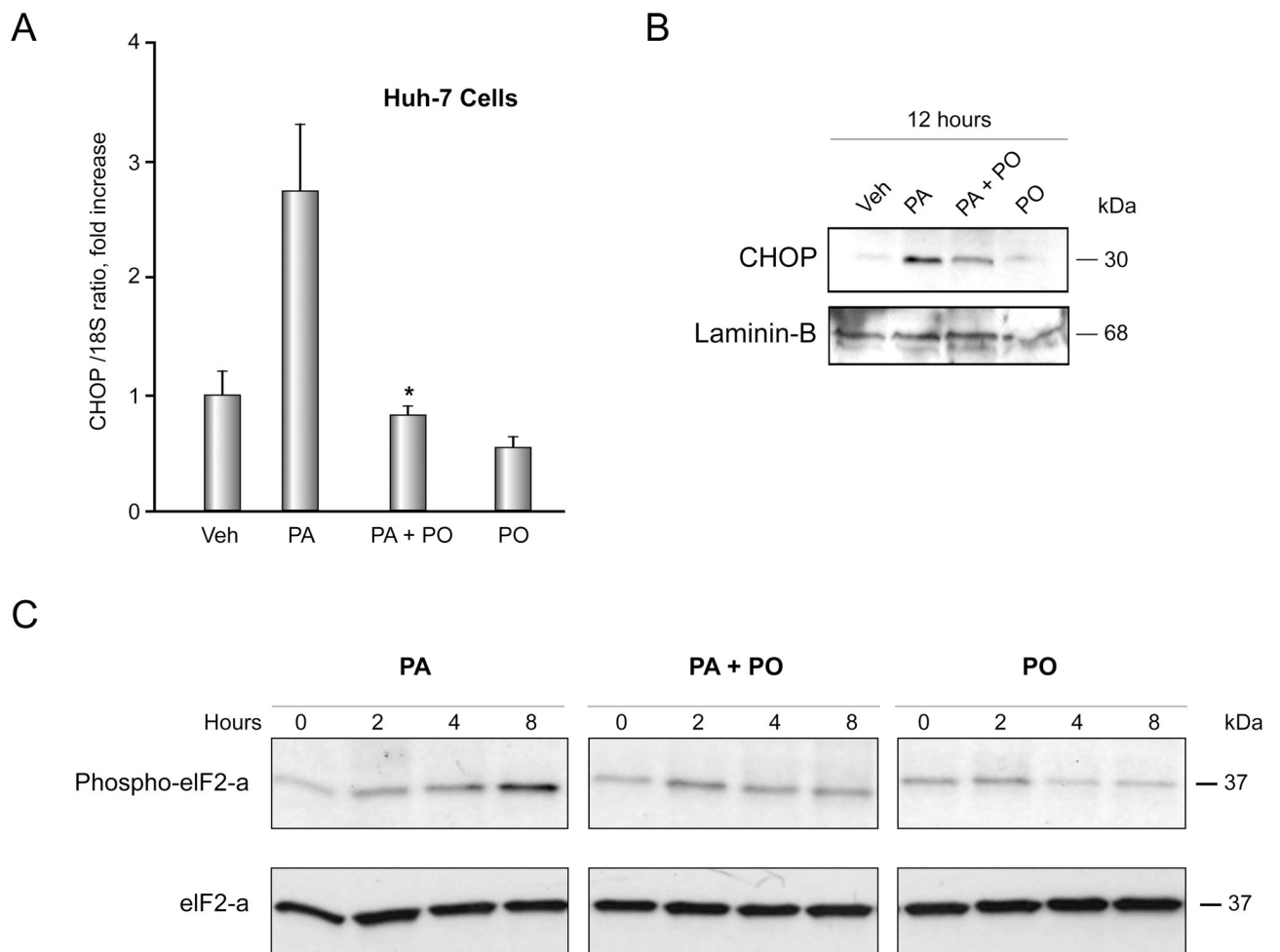


**Figure 3. PO inhibits PA-induced CHOP up-regulation and phosphorylation of eIF2- $\alpha$**   
 (A) Huh-7 cells were treated with vehicle (Veh), 800  $\mu$ M PA, 800  $\mu$ M PA plus 400  $\mu$ M PO, or 400  $\mu$ M PO PO alone for 8 hours. CHOP mRNA was quantified by real time PCR. Fold induction was determined by normalization to 18S. Data represent the mean and error of 3 independent experiments each performed in triplicate. \*  $p < 0.05$ , PA-treated cells vs. PA plus PO-treated cells. (B) Huh-7 cells were treated as above. Nuclear extracts were obtained from each experimental conditions and were subjected to immunoblot analysis for CHOP. Laminin B was used as a loading control. (C) Huh-7 cells were treated as above for the indicated time. Whole cell lysates were obtained and resolved by SDS-PAGE. Proteins were identified by western blot analysis by using antisera specific for total and phospho-eIF2- $\alpha$ .

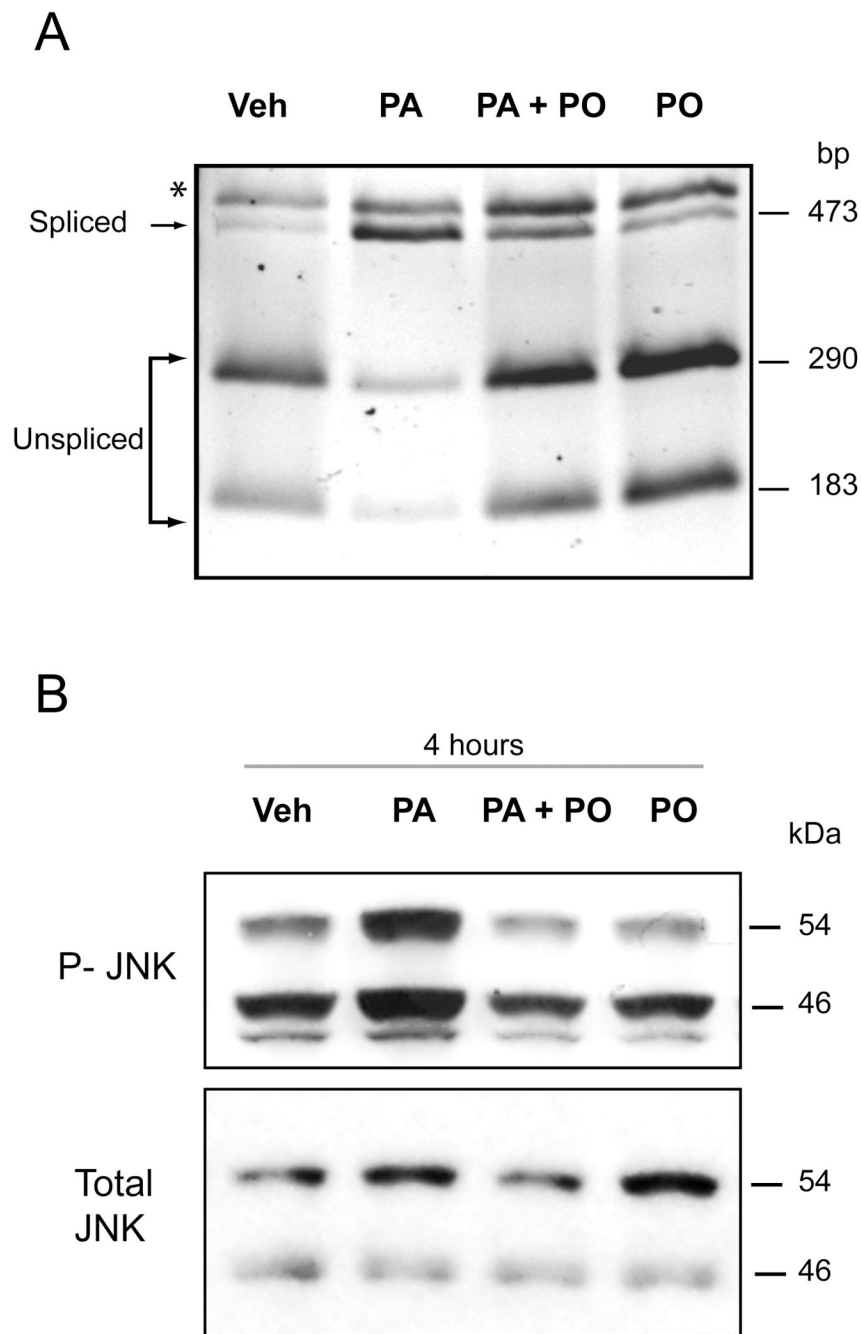


**Figure 4. PO inhibits PA-induced XBP-1 and JNK activation**

(A) Huh-7 cells were treated with either vehicle (Veh), 800  $\mu$ M PA, 800  $\mu$ M PA plus 400  $\mu$ M PO, or 400  $\mu$ M PO alone for 8 hours. XBP-1 cDNA was amplified by PCR followed by 1 hour incubation with Pst1. Unspliced form of XBP-1 shows 290-bp and 180-bp product (which are mainly observed in Veh, PA+PO, PO-treated cells). Spliced form shows single 473-bp amplification product (which is mainly observed in PA-treated cells). \* Undigested PCR product. (B) Huh-7 cells were treated as above for 4 hours. Whole cell lysates were obtained and resolved by SDS-PAGE. Proteins were identified by western blot analysis by using antisera specific for total and active (phospho) members of JNK 1/2.

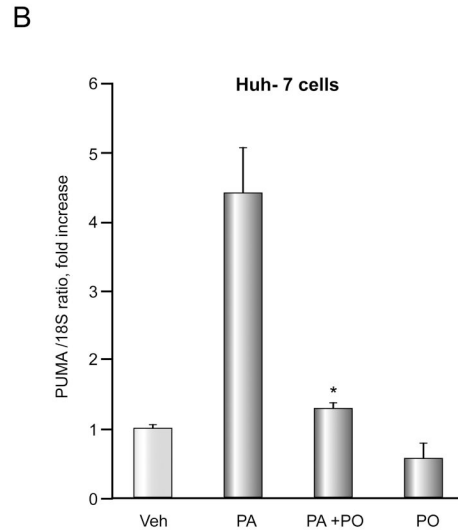
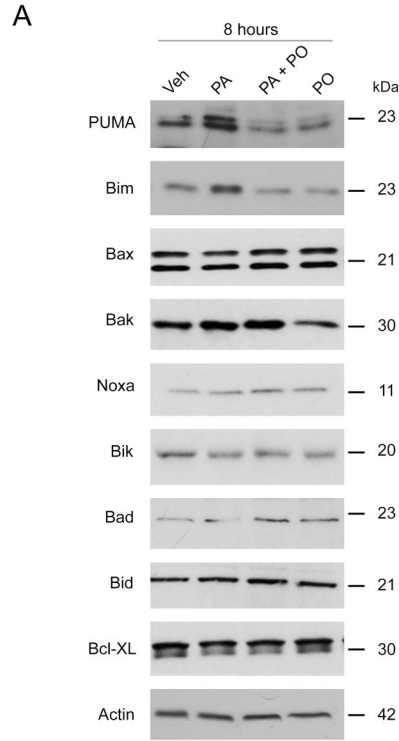


**Figure 5. PO inhibits PA-mediated Bim and PUMA induction and Bax activation**

(A) (A, B) Western blot analysis was performed for Bcl-2 proteins using whole cell lysates from Huh-7 cells treated with vehicle (Veh), 800  $\mu$ M PA, 800  $\mu$ M PA plus 400  $\mu$ M PO, or 400  $\mu$ M PO alone for 8 hours. (B) Huh-7 cells were treated with FFAs as described above. PUMA mRNA was quantified by real time PCR. Fold induction was determined by normalization to 18S. Data represent the mean and error of 3 independent experiments each performed in triplicate. \*  $p < 0.05$ , PA-treated cells vs. PA plus PO-treated cells. (C) Huh-7 cells were examined by immunofluorescence microscopy for activation of Bax following treatment with either vehicle (Veh), 800  $\mu$ M PA, 800  $\mu$ M PA plus 400  $\mu$ M PO, or 400  $\mu$ M PO alone for 16 hours. The primary antibody employed recognizes the N-terminus of Bax which is exposed as

an antigen upon Bax activation. Green fluorescence shows activated Bax and blue fluorescence shows DAPI staining. The graph shows quantification of 5 experiments. \*  $p < 0.01$ , PA-treated cells vs. PA plus PO-treated cells.



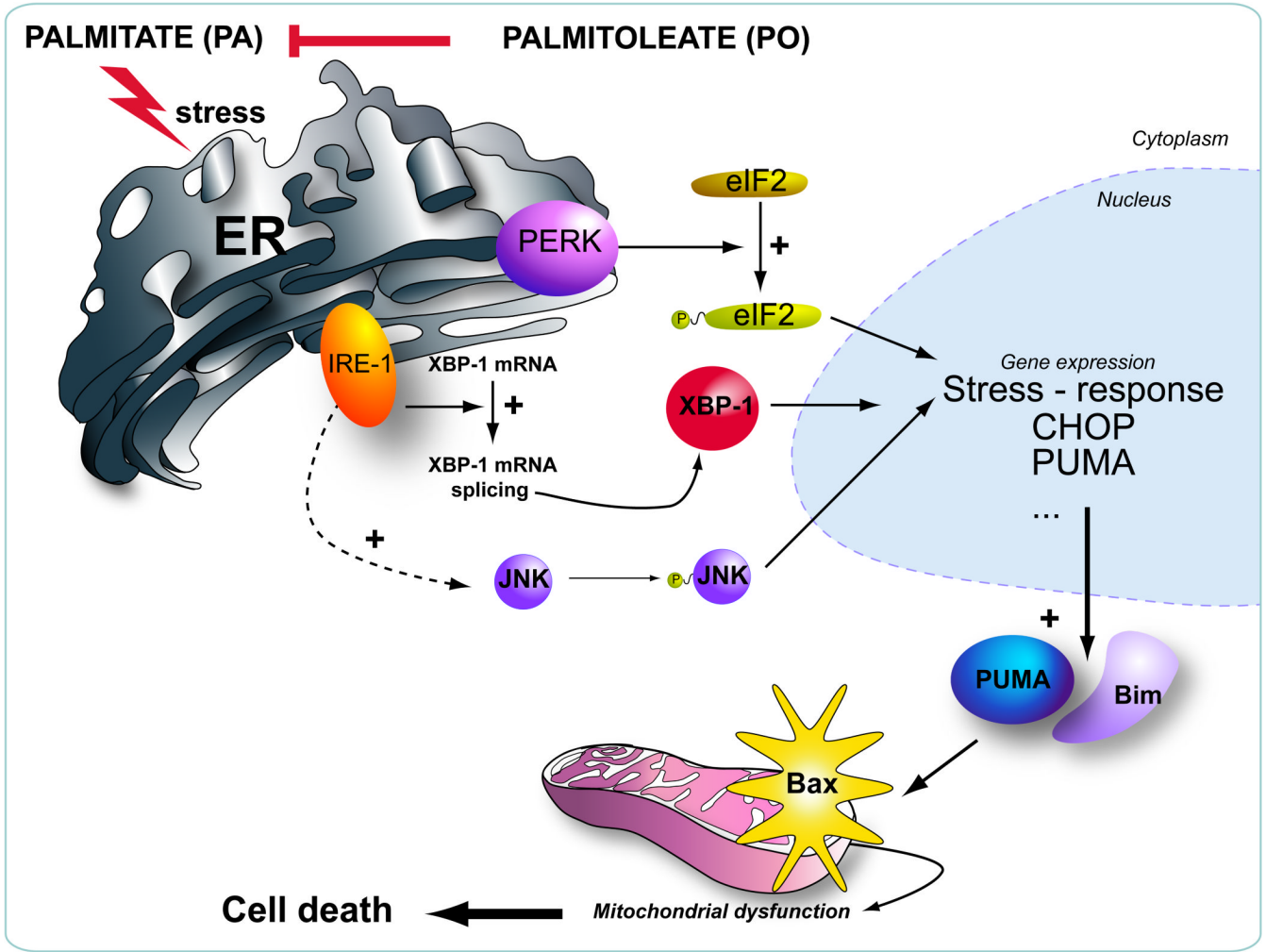


**Figure 6. Schematic representation of the proposed model for the mechanism of PO inhibiting PA-induced apoptosis**  
Palmitoleate (PO) inhibits palmitate (PA)-induced ER stress, thereby preventing induction of the BH3-only proteins PUMA, Bim, and Bax activation.